

Cascading Kalman Observers of Structural Flexible and Wind States for Wind Turbine Control

C.L. Bottasso, A. Croce*

Dipartimento di Ingegneria Aerospaziale, Politecnico di Milano, Milano, Italy

Scientific Report DIA-SR 09-02, Dipartimento di Ingegneria Aerospaziale, Politecnico di Milano, Milano, Italy, January 2009

Abstract

We formulate novel observers of the structural flexible states of a wind turbine, as well as of the wind incident on its rotor.

Stochastic filtering processes reconstruct on-line optimal estimates of the tower and blade states, by using readings from accelerometers and strain gages placed along the structural members. From these reconstructed states, another filtering process estimates the wind states which, improving on the commonly used mean hub-height wind estimates or the point measurements available from on-board anemometers, also include information on the wind-over-the-rotor distribution. The proposed procedure is able to approximate vertical and horizontal wind shear, yawed flow and a vertical wind component.

The instantaneous estimates of the flexible states of tower and blades and of the spatial wind distribution can be used for enabling sophisticated individual-blade fatigue and load alleviating control laws.

The proposed procedures are demonstrated with the help of numerical experiments conducted using a high-fidelity aero-servo-elastic simulator.

1 Introduction

In this work we formulate observers of the structural flexible states of a wind turbine and of the wind blowing on the rotor. The motivation for the proposed observers is to provide estimates of these states to be used by advanced control laws.

For example, knowledge of the tower fore-aft and side-side motions as well as of the blade flapping and lagging can be profitably used for designing sophisticated individual-blade control laws, so as to alleviate fatigue and gust-induced loads. In this work, an assumed modal basis approach is used, and the flexible states reconstructed by the observers are represented by modal amplitudes and velocities of tower and blades. With estimates of these states made available by the proposed observers, one can synthesize model-based control laws which account for the aero-elastic response of such states.

Furthermore, knowledge of the instantaneous wind-over-the-rotor distribution can be exploited so as to explicitly account for this information in the pitch and torque control of a wind turbine. For example, knowledge of the current wind vertical and horizontal shear, as well as of the vertical and lateral wind components can be profitably used for reducing oscillatory loads.

*Corresponding author, Dipartimento di Ingegneria Aerospaziale, Politecnico di Milano, Milano, Via La Masa 34, 20156 Italy. E-mail: carlo.bottasso@polimi.it; Tel.: +39-02-2399-8315; Fax: +39-02-2399-8334.

Clearly, this information is of potential crucial efficacy in the design of control laws since it plays a central role in the determination of the aero-elastic response of the machine; however, the same information on the wind spatial distribution can not be obtained by the on-board anemometer, which can only provide mean hub-height wind values and is also disturbed by interactions with the rotor stream-tube and the nacelle, nor it can be easily obtained by other practical means. Although wind observers have been previously described in the literature [5], these provide only hub-height estimates, i.e. constant-over-the-rotor wind values. While this information is useful and can be profitably used, for example for scheduling the control gains in terms of the wind speed, it does not account for important effects on the aero-elastic response of the wind turbine due to wind non-uniformity. The proposed wind observer tries to remove these limitations, by reconstructing a more complete picture of the instantaneous wind-over-the-rotor distribution.

In the proposed approach, estimates of all unknown states are obtained by a cascading series of Kalman filters. A first filter is responsible for the reconstruction of the tower states. A set of governing equations is obtained by expressing the accelerations sensed by accelerometers placed along the tower in terms of an assumed modal basis. At each time instant, the filter first predicts the tower flexible states by integrating forward in time the governing equations, and then corrects the predictions using the readings of a set of strain gages, also placed along the tower length. This filtering approach accounts for the presence of noise in the measurements of both the accelerometers and the strain gages. For reducing the need for tuning of the filter covariance matrices, an adaptive filtering approach is used, which reconstructs the noise statistics by keeping in memory a buffer of past values.

A second set of parallel filters operates in series to the tower filter, with the goal of reconstructing the flexible blade states. For each blade, the accelerations sensed by accelerometers placed along the blade span are expressed in terms of the assumed modes of the blade, and of the accelerations transmitted by the tower; this last piece of information is at this stage known from the first filter. The filters predict the flexible blade states by integrating forward in time the resulting equations of motion, and then correcting the predictions based on readings provided by strain gages.

The filters are formulated so as to be able to operate with an arbitrary number of sensors, under the constraint of observability of the reconstructed states. However, to keep the number of necessary sensors to a minimum, which is important for reasons of simplicity, the filters can operate with one accelerometer and one strain gage for the tower and for each blade, which is a practical configuration already available on many instrumented wind turbines.

A wind state estimator is here formulated by considering that the flexible rotor of a wind turbine is a sophisticated “sensor” which spans the rotor disk and responds to the temporal and spatial variations of the wind blowing on it. By proper interpretation of the turbine response, one can infer the wind blowing on the rotor. In this work, the spatial wind distribution is approximated using a simple model which accounts for mean hub wind, vertical and lateral shear, wind direction and vertical wind component. These unknown wind parameters are promoted to the role of dynamical states and are identified on-line using a third adaptive filter operating in series with the tower and blade ones. To this end, we use a wind turbine reduced model which accounts for the coupled dynamic equilibrium of drive-train, tower fore-aft and side-side motion, and elastic blade motion. At each instant of time, an adaptive extended Kalman filter estimates the wind states by enforcing in a stochastically optimal sense the satisfaction of the reduced model dynamic equilibrium equations. This is obtained by regarding the wind states as the sole unknowns of the model governing equations, whereas all control inputs and states are either available by readings of the on-board sensors or known through the estimates provided by the structural flexible state observers.

The proposed methodology is demonstrated by using a high fidelity simulation environment, which includes an aero-servo-elastic wind turbine multibody model of the plant, models of the wind, of the sensors, of the actuators and of measurement and process noise. Extensive simulations in gusty and turbulent wind conditions demonstrate the ability of the proposed observers to identify with good accuracy both the flexible response of the machine and the spatial characteristics of the wind.

2 Formulation of the Observers

2.1 Notation

A generic triad is indicated as $\mathcal{A} = (\mathbf{a}_1, \mathbf{a}_2, \mathbf{a}_3)$ and centered at point A , where \mathbf{a}_i , $i = 1, 2, 3$, are mutually orthogonal unit vectors.

The notation $(\cdot)^{\mathcal{A}}$ denotes components of a vector or tensor in triad \mathcal{A} . If $\mathbf{R}_{\mathcal{A} \rightarrow \mathcal{B}}$ is the rotation tensor which brings triad \mathcal{A} into triad \mathcal{B} , then the components of a generic vector \mathbf{v} in the two triads are related as $\mathbf{v}^{\mathcal{A}} = \boldsymbol{\alpha} \mathbf{v}^{\mathcal{B}}$, $\mathbf{v}^{\mathcal{B}} = \boldsymbol{\alpha}^T \mathbf{v}^{\mathcal{A}}$, where $\boldsymbol{\alpha}$ is the direction cosine matrix, $\boldsymbol{\alpha} = \mathbf{R}_{\mathcal{A} \rightarrow \mathcal{B}}^{\mathcal{A}} = \mathbf{R}_{\mathcal{A} \rightarrow \mathcal{B}}^{\mathcal{B}}$, $\boldsymbol{\alpha}^T \boldsymbol{\alpha} = \mathbf{I}$. Since the components of tensor $\mathbf{R}_{\mathcal{A} \rightarrow \mathcal{B}}$ are the same when measured in either \mathcal{A} or \mathcal{B} , we typically avoid the use of the component superscript for rotation tensors, unless its components are measured in a triad other than \mathcal{A} or \mathcal{B} .

The notation \mathbf{v}_{\times} is used to indicate the skew-symmetric tensor associated with vector \mathbf{v} , and $(\cdot)^T$ to indicate the transpose operation.

The symbol $(\dot{\cdot}) = d \cdot / dt$ indicates a derivative with respect to time t , while the symbol $(\cdot)' = d \cdot / d\xi$ indicates a derivative with respect to the curvilinear coordinate $\xi \in [0, L]$ measured along the beam reference line, L being the beam length.

The angular velocity of triad \mathcal{B} with respect to triad \mathcal{A} is noted $\boldsymbol{\omega}_{\mathcal{B}/\mathcal{A}}$, where $\dot{\mathbf{R}}_{\mathcal{A} \rightarrow \mathcal{B}} = \boldsymbol{\omega}_{\mathcal{B}/\mathcal{A}} \times \mathbf{R}_{\mathcal{A} \rightarrow \mathcal{B}}$. The curvature of triad \mathcal{B} with respect to triad \mathcal{A} is noted $\mathbf{c}_{\mathcal{B}/\mathcal{A}}$, where $\mathbf{R}'_{\mathcal{A} \rightarrow \mathcal{B}} = \mathbf{c}_{\mathcal{B}/\mathcal{A}} \times \mathbf{R}_{\mathcal{A} \rightarrow \mathcal{B}}$.

2.2 Observer of Structural Flexible States of a Wind Turbine

2.2.1 Tower State Observer

A tower state observer is here formulated by first expressing the accelerations sensed by accelerometers placed along the tower in terms of unknown modal states. The solution of the resulting equations of motion results in predicted modal states, which are then corrected based on the readings provided by strain gages. This prediction-correction approach is implemented by a Kalman filter which accounts for noise in the measurements.

Consider the wind turbine tower depicted in Fig. 1. An accelerometer is placed on the tower at a location identified by the abscissa ξ_P measured along the tower axis. The undeformed tower configuration at that location along the span is described in terms of a local body-attached triad \mathcal{P}_0 centered at point P_0 , while the deformed tower configuration is described by a body-attached triad \mathcal{P} centered at point P . Furthermore, an inertial frame of reference is denoted by a triad of unit vectors \mathcal{I} centered at point I .

The components of the acceleration in the body-attached frame, $\mathbf{a}_{P/\mathcal{I}}^{\mathcal{P}}$, are sensed by the

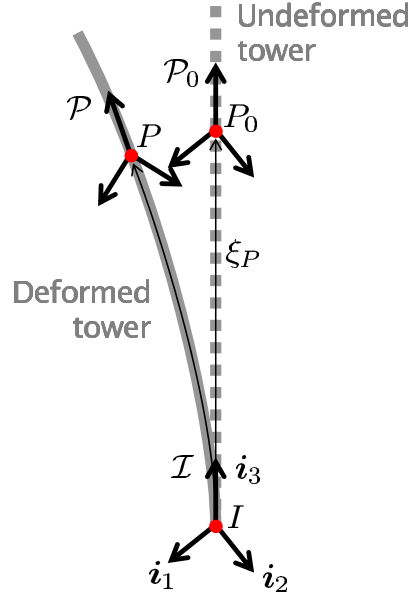


Fig. 1: Reference frames for the tower observer.

accelerometer which yields a reading $\mathbf{a}_{\text{acc } P}$ affected by noise \mathbf{m}_{acc} ¹:

$$\mathbf{a}_{\text{acc } P} = \mathbf{a}_{P/I}^{\mathcal{P}} + \mathbf{m}_{\text{acc}}. \quad (2)$$

The tower deformation is now modeled using N assumed mode shapes, whose components in \mathcal{I} we assume to have been obtained by using some finite element software. This way, the inertial acceleration components at the accelerometer location can be computed as

$$\mathbf{a}_{P/I}^{\mathcal{I}} = \sum_{i=1}^N \Phi_i^{\mathcal{I}}(\xi_P) \dot{v}_i, \quad (3)$$

where $\Phi_i^{\mathcal{I}}(\xi)$ are the components in \mathcal{I} of the i th tower displacement mode shape, q_i its associated unknown modal amplitude and $v_i = \dot{q}_i$ the unknown modal velocity.

On the other hand, the components of the acceleration vector in the inertial frame can also be written as

$$\mathbf{a}_{P/I}^{\mathcal{I}} = \mathbf{R}_{\mathcal{I} \rightarrow \mathcal{P}} \mathbf{a}_{P/I}^{\mathcal{P}}, \quad (4)$$

where the rotation tensor from triad \mathcal{I} to triad \mathcal{P} is

$$\mathbf{R}_{\mathcal{I} \rightarrow \mathcal{P}} = \mathbf{R}_{\mathcal{P}_0 \rightarrow \mathcal{P}} \mathbf{R}_{\mathcal{I} \rightarrow \mathcal{P}_0}. \quad (5)$$

¹ Notice that, when using an accelerometer located in the nacelle, the sensed acceleration components are

$$\mathbf{a}_{\text{acc } P} = \mathbf{a}_{P/I}^{\mathcal{Y}} + \mathbf{m}_{\text{acc}}, \quad (1)$$

where \mathcal{Y} is the nacelle-attached yawing triad, which are however readily transformed into the \mathcal{P} triad as $\mathbf{a}_{P/I}^{\mathcal{P}} = \mathbf{R}_{\mathcal{P} \rightarrow \mathcal{Y}}^{\mathcal{P}} \mathbf{a}_{P/I}^{\mathcal{Y}}$, $\mathbf{R}_{\mathcal{P} \rightarrow \mathcal{Y}}$ being a planar rotation of yaw angle θ about the \mathbf{t}_3 axis (see description of reference frames in §2.2.3 and cf. Fig. 2).

For a straight tower, as it is often the case, the rotation tensor from the inertial to the undeformed frame is $\mathbf{R}_{\mathcal{I} \rightarrow \mathcal{P}_0} = \mathbf{I}$. Furthermore, the relative rotation tensor which accounts for the tower deformation, given that mode shapes describe small motions about the reference configuration, can be expressed in the following linear form

$$\mathbf{R}_{\mathcal{P}_0 \rightarrow \mathcal{P}}^{\mathcal{I}} = \mathbf{I} + \left(\sum_{i=1}^N \Theta_i^{\mathcal{I}}(\xi_P) q_i \right)_{\times}, \quad (6)$$

where $\Theta_i^{\mathcal{I}}(\xi)$ are the components in \mathcal{I} of the i th tower rotation mode shape. For shear undeformable beams, the rotational modes are simply the derivatives of the displacement modes with respect to the curvilinear abscissa ξ .

Using now (3) and (4), together with the given definitions of sensed acceleration and rotation tensors, we obtain the acceleration components at point P as

$$\sum_{i=1}^N \Phi_i^{\mathcal{I}}(\xi_P) \dot{v}_i = \left(\mathbf{I} + \left(\sum_{i=1}^N \Theta_i^{\mathcal{I}}(\xi_P) q_i \right)_{\times} \right) \mathbf{R}_{\mathcal{I} \rightarrow \mathcal{P}_0} (\mathbf{a}_{\text{acc } P} - \mathbf{m}_{\text{acc}}). \quad (7)$$

Consider now N_{acc} accelerometers located in the set of points S_{acc} , and define the $3N_{\text{acc}} \times N$ matrix

$$\mathbf{A} = [\Phi_i^{\mathcal{I}}(\xi_P)], \quad P \in S_{\text{acc}}, \quad i = 1, \dots, N_{\text{acc}}, \quad (8)$$

and the $3N_{\text{acc}} \times 1$ vector $\mathbf{a} = (\dots, \mathbf{a}_{P/\mathcal{I}}^{\mathcal{I}}, \dots)^T$ with $P \in S_{\text{acc}}$, where the expression for $\mathbf{a}_{P/\mathcal{I}}^{\mathcal{I}}$ is given by the right hand side of (7). Defining the modal amplitude $\mathbf{q} = (\dots, q_i, \dots)^T$ and velocity $\mathbf{v} = (\dots, v_i, \dots)^T$ vectors, the modal equations of motion are obtained using least-squares on (7) as

$$\dot{\mathbf{q}} = \mathbf{v}, \quad (9a)$$

$$\dot{\mathbf{v}} = (\mathbf{A}^T \mathbf{A})^{-1} \mathbf{A} \mathbf{a}. \quad (9b)$$

Consider now a strain gage placed at a location identified by the abscissa ξ_Q along the tower axis. The body-attached triads in the reference and deformed configurations are \mathcal{Q}_0 centered at Q_0 and \mathcal{Q} centered at Q , respectively. The curvature components in \mathcal{I} of the deformed beam at that location are

$$\mathbf{c}_{\mathcal{Q}/\mathcal{I}}^{\mathcal{I}} = \mathbf{c}_{\mathcal{Q}_0/\mathcal{I}}^{\mathcal{I}} + \mathbf{c}_{\mathcal{Q}/\mathcal{Q}_0}^{\mathcal{I}}, \quad (10)$$

where the curvature due to the tower deformation can be expressed as

$$\mathbf{c}_{\mathcal{Q}/\mathcal{Q}_0}^{\mathcal{I}} = \sum_{i=1}^N \Theta_i^{\mathcal{I}}(\xi_Q) q_i. \quad (11)$$

On the other hand, the same curvature components can be computed as

$$\mathbf{c}_{\mathcal{Q}/\mathcal{Q}_0}^{\mathcal{I}} = \mathbf{R}_{\mathcal{I} \rightarrow \mathcal{Q}} \mathbf{c}_{\mathcal{Q}/\mathcal{Q}_0}^{\mathcal{Q}}, \quad (12a)$$

$$= \left(\mathbf{I} + \left(\sum_{i=1}^N \Theta_i^{\mathcal{I}}(\xi_Q) q_i \right)_{\times} \right) \mathbf{R}_{\mathcal{I} \rightarrow \mathcal{Q}_0} \mathbf{c}_{\mathcal{Q}/\mathcal{Q}_0}^{\mathcal{Q}}, \quad (12b)$$

so that the local body-attached curvature components are

$$\mathbf{c}_{\mathcal{Q}/\mathcal{Q}_0}^{\mathcal{Q}} = \mathbf{R}_{\mathcal{I} \rightarrow \mathcal{Q}_0}^T \left(\mathbf{I} + \left(\sum_{i=1}^N \boldsymbol{\Theta}_i^T(\xi_Q) q_i \right)_{\times} \right)^{-1} \sum_{i=1}^N \boldsymbol{\Theta}_i^T(\xi_Q) q_i. \quad (13)$$

These components are sensed by the strain gage which yields a reading $\mathbf{c}_{\text{sg}Q}$ affected by noise \mathbf{n}_{sg} , i.e.:

$$\mathbf{c}_{\text{sg}Q} = \mathbf{c}_{\mathcal{Q}/\mathcal{Q}_0}^{\mathcal{Q}} + \mathbf{n}_{\text{sg}}. \quad (14)$$

Considering N_{sg} strain gages located in the set of points S_{sg} , we can define the $3N_{\text{sg}} \times 1$ output vector

$$\mathbf{y} = (\dots, \mathbf{c}_{\mathcal{Q}/\mathcal{Q}_0}^{\mathcal{Q}T}, \dots)^T, \quad Q \in S_{\text{sg}}, \quad (15)$$

where the expression for $\mathbf{c}_{\mathcal{Q}/\mathcal{Q}_0}^{\mathcal{Q}}$ is given in (13), and measurement vector

$$\mathbf{z} = (\dots, \mathbf{c}_{\text{sg}Q}^T, \dots)^T, \quad Q \in S_{\text{sg}}. \quad (16)$$

The equations of motion (9) together with the output and measurement definitions (15,16) represent a set of state-space equations for the tower observer, which can be written in the following compact form

$$\dot{\mathbf{x}} = \mathbf{f}(\mathbf{x}, \mathbf{u}, \mathbf{m}), \quad (17a)$$

$$\mathbf{y} = \mathbf{h}(\mathbf{x}), \quad (17b)$$

$$\mathbf{z} = \mathbf{y} + \mathbf{n}, \quad (17c)$$

where the state vector is $\mathbf{x} = (\mathbf{q}^T, \mathbf{v}^T)^T$, the input vector $\mathbf{u} = (\dots, \mathbf{a}_{\text{acc}P}^T, \dots)^T$ with $P \in S_{\text{acc}}$, the process noise vector $\mathbf{m} = \mathbf{m}_{\text{acc}}$ (which here is in reality due to the accelerometer measurement noise), and the (strain gage) measurement noise vector $\mathbf{n} = \mathbf{n}_{\text{sg}}$.

2.2.2 State Estimation by Adaptive Kalman Filtering

The state estimation problem (17) can be solved with a number of filtering approaches. The Kalman filter is an optimal estimator for unconstrained linear systems with normally distributed process and measurement noise, while for non-linear problem various methods have been proposed, including the extended Kalman filter, the unscented Kalman filter, the sigma point and particle filters [10]. In this work we use the extended Kalman filter, which amounts to an approximate generalization of the Kalman filter to non-linear systems obtained by linearizing the system dynamics at each time step. Theoretical results on the stability and convergence of this approach are discussed in Ref. [8].

The equations of motion (17a) are integrated on each sampling interval $[t_k, t_{k+1}]$ to yield a state prediction $\bar{\mathbf{x}}_{k+1}$ together with its associated output vector $\bar{\mathbf{y}}_{k+1}$ from (17b). Next, at each sampling instant the state predictions are improved based on the innovations, i.e. the difference between the measurements \mathbf{z}_{k+1} and the predicted outputs $\bar{\mathbf{y}}_{k+1}$, as

$$\hat{\mathbf{x}}_{k+1} = \bar{\mathbf{x}}_{k+1} + \mathbf{K}_{k+1} (\mathbf{z}_{k+1} - \bar{\mathbf{y}}_{k+1}), \quad (18)$$

where \mathbf{K}_{k+1} is a time-varying gain matrix, which is propagated forward in time together with the state estimates based on the covariances of the estimation error, and of the process and measurement noise.

The latter two quantities are crucial parameters which govern the convergence behavior of the filter. To alleviate the need for careful tuning of these parameters, we use in this work an adaptive filtering method. The basic idea is in this case to reconstruct on-line during filtering the process and measurement noise statistics, keeping a buffer of past values to extract noise samples [6].

In our implementation, the measurement time histories are preprocessed using zero-phase digital filtering [7] before being passed to the Kalman filter, so as to remove the frequency components which are outside of the band of the adopted modal basis.

2.2.3 Rotor State Observer

A rotor state observer is formulated similarly to the tower state observer. First, for each blade, the accelerations sensed by accelerometers placed along the blade span are expressed in terms of unknown blade modal states. These accelerations also depend on the tower states, which are however known from the previously described computational procedure; therefore, the rotor state observers operate in series with the tower observer. The integration of the resulting equations of motion provide predictions of the blade modal states. Next, the predictions are corrected by using the readings provided by strain gages placed along the blade span, using a Kalman filter.

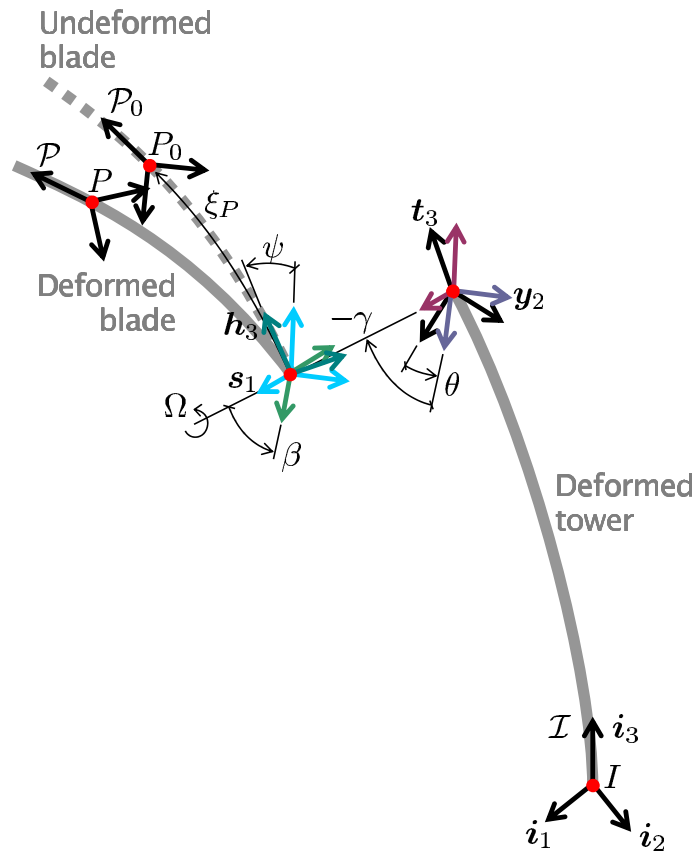


Fig. 2: Reference frames for the blade observer.

Consider the wind turbine schematic configuration depicted in Fig. 2, where a single blade is shown for clarity. An accelerometer is placed on the blade at a location identified by the abscissa ξ_P measured along the blade axis. Similarly to the tower case, in order to express the acceleration

at that location, it is necessary to describe the blade configuration with the help of a cascading series of frames of reference, which are described next. The known tower states are indicated with the notation \hat{q}_{t_i} and \hat{v}_{t_i} , where the subscript $(\cdot)_t$ is used now to indicate tower quantities and the subscript $(\cdot)_b$ for blade related ones.

1. At the tip of the tower, a tower-attached triad \mathcal{T}_0 centered at point T_0 describes the tower tip undeformed configuration, with $\mathbf{R}_{\mathcal{T} \rightarrow \mathcal{T}_0} = \mathbf{I}$ for a straight tower.
2. The deformed tower configuration is described by triad \mathcal{T} centered at point T , where

$$\mathbf{r}_{T_0 T}^{\mathcal{T}} = \sum_{i=1}^{N_t} \Phi_{t_i}^{\mathcal{T}}(\xi_T) \hat{q}_{t_i}, \quad (19a)$$

$$\mathbf{R}_{\mathcal{T}_0 \rightarrow \mathcal{T}}^{\mathcal{T}} = \mathbf{I} + \left(\sum_{i=1}^{N_t} \Theta_{t_i}^{\mathcal{T}}(\xi_T) \hat{q}_{t_i} \right)_{\times}. \quad (19b)$$

3. The yawing nacelle-attached triad $\mathcal{Y} = (\mathbf{y}_1, \mathbf{y}_2, \mathbf{y}_3)$ is centered at $Y \equiv T$ and it is obtained from the \mathcal{T} triad through a planar rotation of yaw angle θ about axis \mathbf{t}_3 .
4. The shaft-parallel nacelle-fixed triad $\mathcal{S} = (\mathbf{s}_1, \mathbf{s}_2, \mathbf{s}_3)$ is obtained from the \mathcal{Y} triad through a planar rotation of angle $-\gamma$ about the \mathbf{y}_2 axis, where γ is the rotor up-tilt angle.
5. The hub-fixed rotating triad $\mathcal{H} = (\mathbf{h}_1, \mathbf{h}_2, \mathbf{h}_3)$ is obtained from the \mathcal{S} one by a planar rotation of azimuthal angle ψ about the \mathbf{s}_1 axis, and centered at point H .
6. The blade-root-fixed triad $\mathcal{B} = (\mathbf{b}_1, \mathbf{b}_2, \mathbf{b}_3)$ is obtained from the \mathcal{H} triad by a planar rotation of blade pitch angle β about the \mathbf{h}_3 axis, and centered at point $B \equiv H$.
7. The undeformed blade configuration is described in terms of a local body-attached triad \mathcal{P}_0 centered at point P_0 . The rotation $\mathbf{R}_{\mathcal{B} \rightarrow \mathcal{P}_0}$ accounts for blade pre-cone, twist and sweep at that location along the blade span.
8. Finally, the deformed blade configuration is described by a body-attached triad \mathcal{P} centered at point P . The blade deformation is modeled using N_b assumed mode shapes, whose components in the blade-root pitching triad \mathcal{B} we assume to have been obtained by using some finite element software. The relative displacement and rotation components accounting for blade deformation are, respectively,

$$\mathbf{r}_{P_0 P}^{\mathcal{B}} = \sum_{i=1}^{N_b} \Phi_{b_i}^{\mathcal{B}}(\xi_P) q_{b_i}, \quad (20a)$$

$$\mathbf{R}_{\mathcal{P}_0 \rightarrow \mathcal{P}}^{\mathcal{B}} = \mathbf{I} + \left(\sum_{i=1}^{N_b} \Theta_{b_i}^{\mathcal{B}}(\xi_P) q_{b_i} \right)_{\times}, \quad (20b)$$

where $\Phi_{b_i}^{\mathcal{B}}(\xi)$ and $\Theta_{b_i}^{\mathcal{B}}(\xi)$ are the components in \mathcal{B} of the i th blade displacement and rotation mode shape, respectively, and q_{b_i} the associated unknown modal amplitude.

We assume that the nacelle yaw angle θ , rotor azimuth ψ and blade pitch β are known at each instant of time from on-board sensors, together with their times rate of change, possibly obtained by finite differences.

Similarly to the tower case, the components of the acceleration in the body-attached frame, $\mathbf{a}_{P/I}^{\mathcal{P}}$, are sensed by the blade accelerometer which yields a reading $\mathbf{a}_{\text{acc } P}$ affected by noise \mathbf{m}_{acc} :

$$\mathbf{a}_{\text{acc } P} = \mathbf{a}_{P/I}^{\mathcal{P}} + \mathbf{m}_{\text{acc}}. \quad (21)$$

Since the blade mode shapes are computed in the blade-pitching triad \mathcal{B} , it is convenient to express the acceleration in that same triad, which, given the cascading reference frame definitions above, can be written as

$$\mathbf{a}_{P/I}^{\mathcal{B}} = \mathbf{a}_{B/I}^{\mathcal{B}} + \mathbf{a}_{P/B}^{\mathcal{B}} + 2\boldsymbol{\omega}_{B/I}^{\mathcal{B}} \times \mathbf{v}_{P/B}^{\mathcal{B}} + (\dot{\boldsymbol{\omega}}_{B/I}^{\mathcal{B}} \times + \boldsymbol{\omega}_{B/I}^{\mathcal{B}} \times \boldsymbol{\omega}_{B/I}^{\mathcal{B}}) \mathbf{r}_{BP}^{\mathcal{B}}. \quad (22)$$

The term $\mathbf{a}_{B/I}^{\mathcal{B}}$ can be readily expressed in terms of known tower quantities as

$$\mathbf{a}_{B/I}^{\mathcal{B}} = \mathbf{R}_{I \rightarrow \mathcal{B}}^T \left(\sum_{i=1}^{N_t} \boldsymbol{\Phi}_{t_i}^I(\xi_T) \dot{v}_{t_i} + (\dot{\boldsymbol{\omega}}_{Y/I}^I + \boldsymbol{\omega}_{Y/I}^I \times \boldsymbol{\omega}_{Y/I}^I) \mathbf{R}_{I \rightarrow Y} \mathbf{r}_{YH}^Y \right), \quad (23)$$

where

$$\boldsymbol{\omega}_{Y/I}^I = \sum_{i=1}^{N_t} \boldsymbol{\Theta}_{t_i}^I \hat{v}_{t_i} + \dot{\theta} \mathbf{R}_{I \rightarrow Y} \begin{pmatrix} 0 \\ 0 \\ 1 \end{pmatrix}, \quad (24)$$

and the rotation tensor components are

$$\mathbf{R}_{I \rightarrow Y} = \left(\mathbf{I} + \left(\sum_{i=1}^{N_t} \boldsymbol{\Theta}_{t_i}^I(\xi_T) \hat{q}_{t_i} \right)_{\times} \right) \mathbf{R}_{I \rightarrow \mathcal{T}_0} \begin{bmatrix} c\theta & -c\theta & 0 \\ c\theta & s\theta & 0 \\ 0 & 0 & 1 \end{bmatrix}, \quad (25)$$

where $s = \sin$ and $c = \cos$, and

$$\mathbf{R}_{I \rightarrow \mathcal{B}} = \mathbf{R}_{I \rightarrow Y} \mathbf{R}_{Y \rightarrow \mathcal{B}}, \quad (26)$$

with

$$\mathbf{R}_{Y \rightarrow \mathcal{B}} = \begin{bmatrix} c\gamma c\beta - s\gamma s\psi s\beta & -c\gamma s\beta - s\gamma s\psi c\beta & -s\gamma c\psi \\ c\psi s\beta & c\psi c\beta & -s\psi \\ s\gamma c\beta + c\gamma s\psi s\beta & -s\gamma s\beta + c\gamma s\psi c\beta & c\gamma c\psi \end{bmatrix}, \quad (27)$$

The terms $\mathbf{v}_{P/B}^{\mathcal{B}}$ and $\mathbf{a}_{P/B}^{\mathcal{B}}$ are simply

$$\mathbf{v}_{P/B}^{\mathcal{B}} = \sum_{i=1}^{N_b} \boldsymbol{\Phi}_{b_i}^{\mathcal{B}}(\xi_P) v_{b_i}, \quad (28a)$$

$$\mathbf{a}_{P/B}^{\mathcal{B}} = \sum_{i=1}^{N_b} \boldsymbol{\Phi}_{b_i}^{\mathcal{B}}(\xi_P) \dot{v}_{b_i}, \quad (28b)$$

whereas the angular velocity $\boldsymbol{\omega}_{B/I}^{\mathcal{B}}$ can be obtained as

$$\boldsymbol{\omega}_{B/I}^{\mathcal{B}} = \dot{\beta} \mathbf{h}_3^{\mathcal{B}} + \Omega \mathbf{R}_{\mathcal{H} \rightarrow \mathcal{B}}^T \mathbf{h}_1^{\mathcal{H}} + \dot{\theta} \mathbf{R}_{T \rightarrow \mathcal{B}}^T \mathbf{t}_3^T + \mathbf{R}_{I \rightarrow \mathcal{B}}^T \sum_{i=1}^{N_t} \boldsymbol{\Theta}_{t_i}^I(\xi_T) \hat{v}_{t_i}, \quad (29a)$$

$$= \begin{pmatrix} \Omega c\beta + \dot{\theta} (s\gamma c\beta + c\gamma s\psi s\beta) \\ -\Omega s\beta + \dot{\theta} (-s\gamma s\beta + c\gamma s\psi c\beta) \\ \dot{\beta} + \dot{\theta} c\gamma c\psi \end{pmatrix} + \mathbf{R}_{I \rightarrow \mathcal{B}}^T \sum_{i=1}^{N_t} \boldsymbol{\Theta}_{t_i}^I(\xi_T) \hat{v}_{t_i}. \quad (29b)$$

Inserting these expressions into (22), we find

$$\begin{aligned}
\sum_{i=1}^{N_b} \Phi_{b_i}^{\mathcal{B}}(\xi_P) \dot{v}_{b_i} &= -2 \boldsymbol{\omega}_{\mathcal{B}/\mathcal{I}}^{\mathcal{B}} \times \sum_{i=1}^{N_b} \Phi_{b_i}^{\mathcal{B}}(\xi_P) v_{b_i} - \\
&(\dot{\boldsymbol{\omega}}_{\mathcal{B}/\mathcal{I}}^{\mathcal{B}} \times + \boldsymbol{\omega}_{\mathcal{B}/\mathcal{I}}^{\mathcal{B}} \times \boldsymbol{\omega}_{\mathcal{B}/\mathcal{I}}^{\mathcal{B}} \times) (\mathbf{r}_{\mathcal{B}P_0}^{\mathcal{B}} + \sum_{i=1}^{N_b} \Phi_{b_i}^{\mathcal{B}}(\xi_P) q_{b_i}) + \\
&\left(\mathbf{I} + \left(\sum_{i=1}^{N_b} \Theta_{b_i}^{\mathcal{B}}(\xi_P) q_{b_i} \right)_{\times} \right) \mathbf{R}_{\mathcal{B} \rightarrow \mathcal{P}_0} (\mathbf{a}_{\text{acc } P} - \mathbf{m}_{\text{acc}}) - \\
&\mathbf{R}_{\mathcal{I} \rightarrow \mathcal{B}}^T \left(\sum_{i=1}^{N_t} \Phi_{t_i}^{\mathcal{I}}(\xi_T) \dot{v}_{t_i} + (\dot{\boldsymbol{\omega}}_{\mathcal{Y}/\mathcal{I}}^{\mathcal{I}} \times + \boldsymbol{\omega}_{\mathcal{Y}/\mathcal{I}}^{\mathcal{I}} \times \boldsymbol{\omega}_{\mathcal{Y}/\mathcal{I}}^{\mathcal{I}} \times) \mathbf{R}_{\mathcal{I} \rightarrow \mathcal{Y}} \mathbf{r}_{\mathcal{Y}H}^{\mathcal{Y}} \right). \quad (30)
\end{aligned}$$

Similarly to the tower case, consider now $N_{b_{\text{acc}}}$ accelerometers located in the set of points $S_{b_{\text{acc}}}$ on the blade, and define matrix

$$\mathbf{A}_b = [\Phi_{b_i}^{\mathcal{B}}(\xi_P)], \quad P \in S_{b_{\text{acc}}}, \quad i = 1, \dots, N_{b_{\text{acc}}}, \quad (31)$$

and vector $\mathbf{a}_b = (\dots, \mathbf{a}_{P/\mathcal{B}}^{\mathcal{B}T}, \dots)^T$ with $P \in S_{b_{\text{acc}}}$, where the expression for $\mathbf{a}_{P/\mathcal{B}}^{\mathcal{B}}$ is given by the right hand side of (30). Defining the blade modal amplitude $\mathbf{q}_b = (\dots, q_{b_i}, \dots)^T$ and velocity $\mathbf{v}_b = (\dots, v_{b_i}, \dots)^T$ vectors, the modal equations of motion are obtained using least-squares on (30) as

$$\dot{\mathbf{q}}_b = \mathbf{v}_b, \quad (32a)$$

$$\dot{\mathbf{v}}_b = (\mathbf{A}_b^T \mathbf{A}_b)^{-1} \mathbf{A}_b \mathbf{a}_b. \quad (32b)$$

Consider now a strain gage placed at a location identified by the abscissa ξ_Q along the blade axis. As for the tower case, we find here that the local body-attached curvature components are

$$\mathbf{c}_{\mathcal{Q}/\mathcal{Q}_0}^{\mathcal{Q}} = \mathbf{R}_{\mathcal{B} \rightarrow \mathcal{Q}_0}^T \left(\mathbf{I} + \left(\sum_{i=1}^{N_b} \Theta_{b_i}^{\mathcal{B}}(\xi_Q) q_{b_i} \right)_{\times} \right)^{-1} \sum_{i=1}^{N_b} \Theta_{b_i}^{\mathcal{B}}(\xi_Q) q_{b_i}, \quad (33)$$

which are sensed by the strain gage yielding a reading $\mathbf{c}_{\text{sg } Q}$ affected by noise \mathbf{n}_{sg} :

$$\mathbf{c}_{\text{sg } Q} = \mathbf{c}_{\mathcal{Q}/\mathcal{Q}_0}^{\mathcal{Q}} + \mathbf{n}_{\text{sg}}. \quad (34)$$

Considering $N_{b_{\text{sg}}}$ strain gages located in the set of points $S_{b_{\text{sg}}}$ along the blade, we define the output vector

$$\mathbf{y}_b = (\dots, \mathbf{c}_{\mathcal{Q}/\mathcal{Q}_0}^{\mathcal{Q}T}, \dots)^T, \quad Q \in S_{b_{\text{sg}}}, \quad (35)$$

where the expression for $\mathbf{c}_{\mathcal{Q}/\mathcal{Q}_0}^{\mathcal{Q}}$ is given in (33), and measurement vector

$$\mathbf{z}_b = (\dots, \mathbf{c}_{\text{sg } Q}^T, \dots)^T, \quad Q \in S_{b_{\text{sg}}}. \quad (36)$$

The equations of motion (32) together with the output and measurement definitions (35,36) represent a set of state-space equations for the blade observer, which can be written in the following compact form

$$\dot{\mathbf{x}}_b = \mathbf{f}_b(\mathbf{x}_b, \mathbf{u}_b, \mathbf{m}_b), \quad (37a)$$

$$\mathbf{y}_b = \mathbf{h}_b(\mathbf{x}_b), \quad (37b)$$

$$\mathbf{z}_b = \mathbf{y}_b + \mathbf{n}_b, \quad (37c)$$

where the state vector is $\mathbf{x}_b = (\mathbf{q}_b^T, \mathbf{v}_b^T)^T$, the input vector $\mathbf{u}_b = (\dots, \mathbf{a}_{acc P}^T, \dots, \hat{\mathbf{x}}_t^T)^T$ with $P \in S_{b_{acc}}$ and $\hat{\mathbf{x}}_t$ the state estimates provided by the tower filter, the process noise vector $\mathbf{m}_b = \mathbf{m}_{acc}$, and the measurement noise vector $\mathbf{n}_b = \mathbf{n}_{sg}$.

Estimates of the blade states are obtained at each time step using an adaptive Kalman filter with zero-phase pre-filtering of the measurements, exactly as in the tower case. Notice that there is one observer per blade; the blade observers operate in parallel to one another and in series with the tower observer.

2.3 Observer of Wind States

A wind state observer is here formulated by taking advantage of the reconstructed wind turbine states, available from the previously described tower and blade flexible state observers, to obtain time-varying estimates of suitably chosen wind states using a wind turbine model. In fact, a dynamic model of a wind turbine can be expressed in terms of its governing equations as

$$\dot{\mathbf{x}}_{wt} = \mathbf{f}_{wt}(\mathbf{x}_{wt}, \mathbf{u}_{wt}, \mathbf{w}), \quad (38)$$

where \mathbf{x}_{wt} are wind turbine states, \mathbf{u}_{wt} is the wind turbine input vector, and $\mathbf{w} = \mathbf{w}(\mathbf{r}, t)$ the spatially and temporally varying wind vector. Consider now a wind turbine model such that its state vector \mathbf{x}_{wt} is

$$\mathbf{x}_{wt} = (\theta, \dot{\theta}, \psi, \dot{\psi}, \dots, \beta_i, \dot{\beta}_i, \dots, \mathbf{q}_t^T, \mathbf{v}_t^T, \dots, \mathbf{q}_{b_i}^T, \mathbf{v}_{b_i}^T, \dots, T_g)^T, \quad i = 1, \dots, B, \quad (39)$$

where T_g is the generator torque and B the number of blades, whereas the input vector is

$$\mathbf{u}_{wt} = (\theta_c, \dots, \beta_{i_g}, \dots, T_{g_c})^T, \quad i = 1, \dots, B, \quad (40)$$

where θ_c is the commanded yaw angle, β_{i_g} the commanded blade pitch setting and T_{g_c} the commanded generator torque. At each instant of time the states are known, either from sensors or from the observers described above. Similarly, at each instant of time also the inputs are known from the on-board controllers.

Taking advantage of the fact that both states and inputs are known in (38), one can infer the wind \mathbf{w} blowing on the rotor. To this end, it is first necessary to introduce a spatial discretization of the wind. A possible solution is provided by the frequently used wind model given by

$$\mathbf{w}(\mathbf{r}, t) = \left(V_h(t) \left(1 + \frac{z - H}{H} \right)^{V_s(t)} + V_{ls}(t) \frac{z - H}{2R} + H_{ls}(t) \frac{y \cos \alpha(t) - x \sin \alpha(t)}{2R} \right) \mathbf{i}_v(t) + V_z(t) \mathbf{i}_3, \quad (41)$$

where x , y and z are coordinates measured along the unit vectors \mathbf{i}_1 , \mathbf{i}_2 and \mathbf{i}_3 , respectively, of \mathcal{I} . V_h is the horizontal wind speed at the height $z = H$ of the rotor hub, V_s is the vertical-shear power law exponent, V_{ls} and H_{ls} are the vertical and horizontal, respectively, linear shear coefficients, R being the rotor radius. The instantaneous horizontal wind direction is given by unit vector \mathbf{i}_v , which forms an angle $\alpha = \text{acos}(\mathbf{i}_1 \cdot \mathbf{i}_v)$ with unit vector \mathbf{i}_1 of the inertial triad \mathcal{I} , while V_z is the vertical wind component.

Selecting as unknown wind parameters the hub wind V_h , either the power law exponent V_s or the vertical shear coefficient V_{ls} , the horizontal wind shear coefficient H_{ls} , the relative wind direction α and the vertical wind component V_z , we can define the vector

$$\mathbf{x}_{wind}(t) = (V_h(t), V_s(t) | V_{ls}(t), H_{ls}(t), \alpha(t), V_z(t))^T, \quad (42)$$

and write the wind parameterization as $\mathbf{w}(\mathbf{r}, t) = \mathbf{w}(\mathbf{x}_{\text{wind}}(t))$.

Next, the unknown wind parameters \mathbf{x}_{wind} are promoted to the role of states, which transforms their estimation problem into a new state estimation one. The governing wind estimation equations in state-space form are written as

$$\dot{\mathbf{x}}_{\text{wind}} = \mathbf{m}_{\text{wind}}, \quad (43a)$$

$$\mathbf{y}_{\text{wind}} = \mathbf{h}_{\text{wind}}(\mathbf{x}_{\text{wind}}, \mathbf{u}_{\text{wind}}), \quad (43b)$$

$$\mathbf{z}_{\text{wind}} = \mathbf{y}_{\text{wind}} + \mathbf{n}_{\text{wind}}. \quad (43c)$$

Equations (43a) represent the wind parameter dynamics evolution equations, where a process noise term \mathbf{m}_{wind} to the right hand side is responsible for exciting the temporal variations of the wind states. Equations (43b) are the output definition equations, representing the residuals of (38):

$$\mathbf{h}_{\text{wind}}(\mathbf{x}_{\text{wind}}, \mathbf{u}_{\text{wind}}) = (\hat{\mathbf{x}}_{\text{wt}} - \mathbf{f}_{\text{wt}}(\hat{\mathbf{x}}_{\text{wt}}, \mathbf{u}_{\text{wt}}, \mathbf{w}(\mathbf{x}_{\text{wind}})))_{\text{dyn eq}}. \quad (44)$$

Notice that the residuals are evaluated for the known wind turbine state $\hat{\mathbf{x}}_{\text{wt}}$ and known input \mathbf{u}_{wt} vectors, which can therefore be considered as inputs to the wind state-space model, i.e. $\mathbf{u}_{\text{wind}} = (\hat{\mathbf{x}}_{\text{wt}}^T, \mathbf{u}_{\text{wt}}^T)^T$. Furthermore, of the complete set of governing equations (38) represented by dynamic equilibrium and kinematic equations, only the former set depends on the wind \mathbf{w} ; therefore, in (44), only the dynamic equilibrium set of equations enters into the definition of the outputs. Finally, equations (43c) represent the measurement definition equations. For this special problem, the measurements at all time instants are simply

$$\mathbf{z}_{\text{wind}} = \mathbf{0}, \quad (45)$$

which means that we are trying to enforce a null error in the satisfaction of the dynamic equilibrium equations of the wind turbine model. In other words, we are trying to find those wind states which satisfy the dynamic equilibrium equations with the given measured and reconstructed quantities. Notice that a noise term \mathbf{n}_{wind} appears in the measurement definitions; however, in this case this is not a proper measurement noise term but in reality a process noise one, since it appears as an additive term in the dynamic equilibrium equations.

The state estimation problem (43) is solved here again with an adaptive extended Kalman filter. The reconstructed wind states, together with the elastic tower and blade states, can now be used by advanced on-line control laws which this way can explicitly account for this information in their formulation.

The overall architecture of the state estimators is shown in Fig. 3.

3 Results

3.1 Observer of Structural Flexible States

To illustrate the performance of the proposed observer of structural flexible states, we consider here the response of the LTW80 wind turbine [2]. The tests are conducted within a simulation environment, more fully described in Ref. [4]. The virtual plant includes a detailed aero-servo-elastic model of the wind turbine, models of the wind, of the sensors and of the actuators on-board the machine, and it is operated by a control system which includes supervision of operating conditions and active blade pitch-torque control. The aero-servo-elastic model of the wind turbine is implemented with the software **Cp-Lambda** (**C**ode for **P**erformance, **L**oads and **A**eroelasticity by **M**ulti-**B**ody **D**ynamic **A**nalysis), based on a finite-element multibody formulation described in Ref. [3] and references therein.

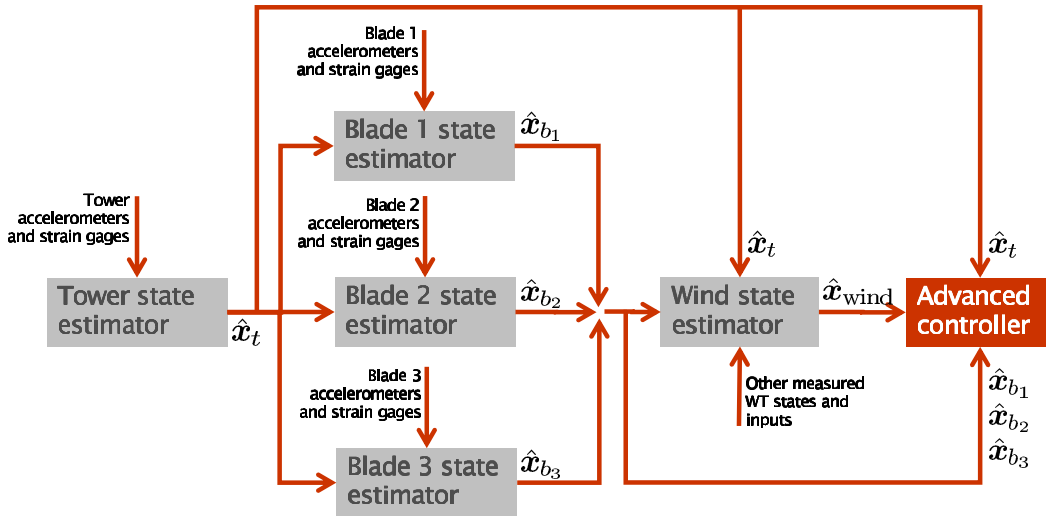


Fig. 3: Overall architecture of the estimators of flexible tower and blade states, and of wind states.

The tower has a strain gage located at $\xi_Q = 60$ m ($L = 77.5$ m), and an accelerometer at its top in the nacelle. Each blade has a strain gage at $\xi_Q = 15$ m ($R = 40$ m), and an accelerometer at $\xi_P = 30$ m. All sensors are affected by errors modeled as white noise with an amplitude not to exceed the 5% of the measured signal. Sensor signals are zero-phase filtered with a 2 Hz pass-band. The adaptive Kalman filters use buffers of 15 past samples to reconstruct on-line the noise statistics.

At first, we consider the case of the extreme operating gust (EOG) at 15 m/sec [1]. Figure 4 shows the time history of the wind, and the resulting rotor angular speed and collective blade pitch (respectively, from top to bottom).

Figure 5 shows, at left, the time history of the blade deflection at the accelerometer location, and at right the time history of the tower tip deflection. The “true” plant response is reported using a solid line, while the observed response is shown using a dashed line. In both cases, but especially for the blade case, it appears that there is an excellent correspondence between the reference and reconstructed states. The only observable inaccuracy is an offset in the peak response of the tower, corresponding to the maximum wind speed during the gust.

Next, we evaluate the performance of the observer in turbulent wind conditions. Transient simulations were conducted for a duration of 600 sec with constant mean hub-height wind speed and Category A turbulence. Figure 6 shows the time history of the turbulent wind in the case of the 11 m/sec mean hub-height wind speed, and the resulting rotor angular speed and collective blade pitch (respectively, from top to bottom).

Figure 7 reports at left the blade deflection time history, and at right the tower tip deflection time history. As in the previous plots, the plant response is reported using a solid line, while the observed response is shown using a dashed line. Here again, the observed deflections match very well the true ones throughout the entire simulation.

3.2 Observer of Wind States

Testing of the wind state observer is still in progress, and here we only show some preliminary results. In the present examples, the reduced model is implemented with the SymDyn software [9],

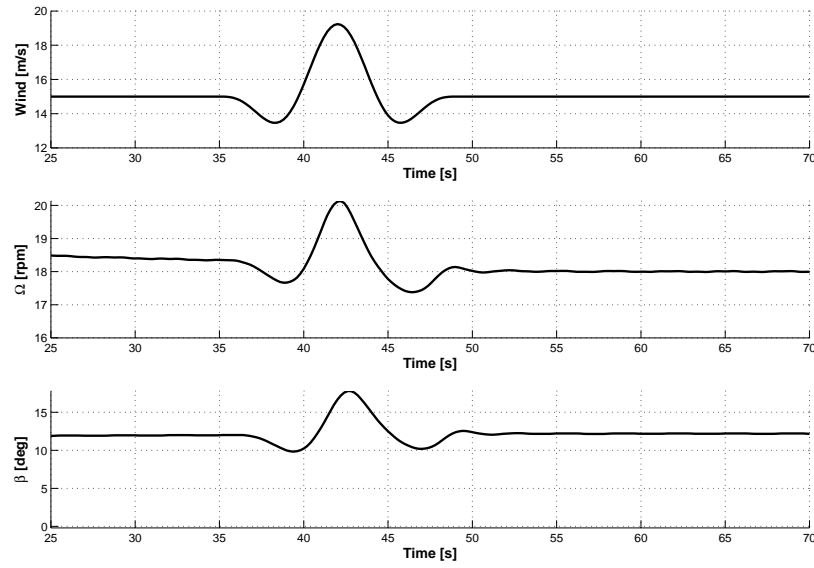


Fig. 4: EOG at 15 m/sec. From top to bottom, time history of wind, rotor angular speed and collective blade pitch.

and the identified modal amplitudes of tower and blades are mapped into equivalent hinge rotations. Time histories of generalized wind states were generated and used for calculating the response of a `SymDyn` model of the LTW80 wind turbine. Horizontal, vertical and lateral wind components were generated using the Kaimal turbulence model, while the vertical shear power law exponent and horizontal wind shear coefficient were varied according to an assumed deterministic time history. Based on this response, estimates of the wind states were obtained using the Kalman observer. Notice that there is no mismatch between plant model and observer model in the results reported below. Consequently, discrepancies between the actual and reconstructed wind states are only due to the presence of noise in the procedure. These preliminary computations were conducted so as to determine the actual observability of the wind states and to verify

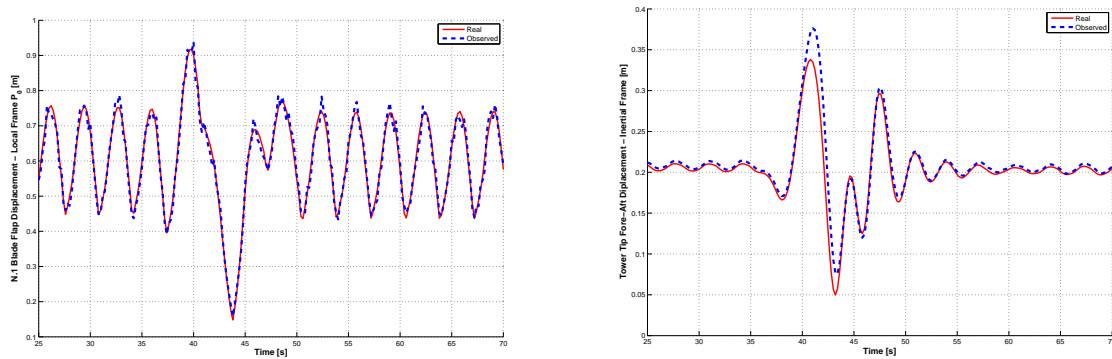


Fig. 5: EOG at 15 m/sec. Time history of blade (left) and tower (right) deflections. Real: solid line; observed: dashed line.

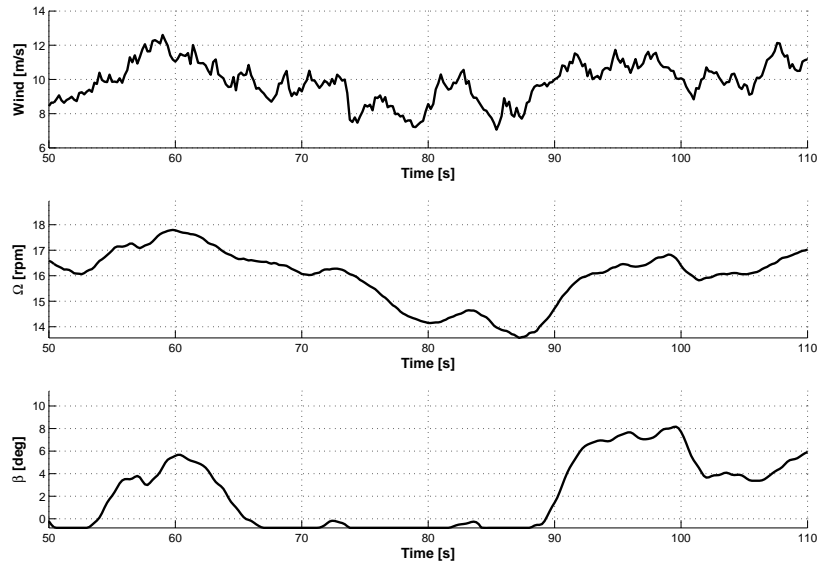


Fig. 6: Turbulent wind with 11 m/sec mean hub-height wind speed and Category A turbulence. From top to bottom, time history of wind, rotor angular speed and collective blade pitch.

the correct implementation of the software. Testing with the response obtained using the fine scale aero-servo-elastic model as plant are currently being conducted and will be documented in a forthcoming publication.

Figure 8 shows at left the time history of the horizontal wind component of Eq. (42), i.e. the hub wind V_h , where the actual wind is reported with a solid line and the reconstructed one using a dashed line. Similarly, the right part of the same figure shows the reconstruction of the power law exponent V_s . Even in this case, the time history of this parameter is captured extremely well by the observer.

Acknowledgements

The authors acknowledge the contribution of D. Devecchi, C.E.D. Riboldi, V. Ronchi and B. Savini in the implementation of the software described in this document and in the development of some of the examples. The first author gratefully acknowledges the hospitality of the National Wind Technology Center, National Renewable Energy Laboratory, Golden, CO, USA, during part of the development of the research described in this paper. Data for the modeling of the LTW80 wind turbine was provided courtesy of the LeitWind company.

References

- [1] Wind Turbines — Part 1: Desing Requirements, Ed. 3.0, *International Standard IEC 61400-1*, 2005.
- [2] LeitWind S.p.A., Via Brennero 34, I-39049 Vipiteno, BZ, Italy, www.leitwind.com.
- [3] O.A. Bauchau, C.L. Bottasso, Y.G. Nikishkov, ‘Modeling Rotorcraft Dynamics with Finite Element Multibody Procedures’, *Mathematics and Computer Modeling*, **33**:1113-1137, 2001.

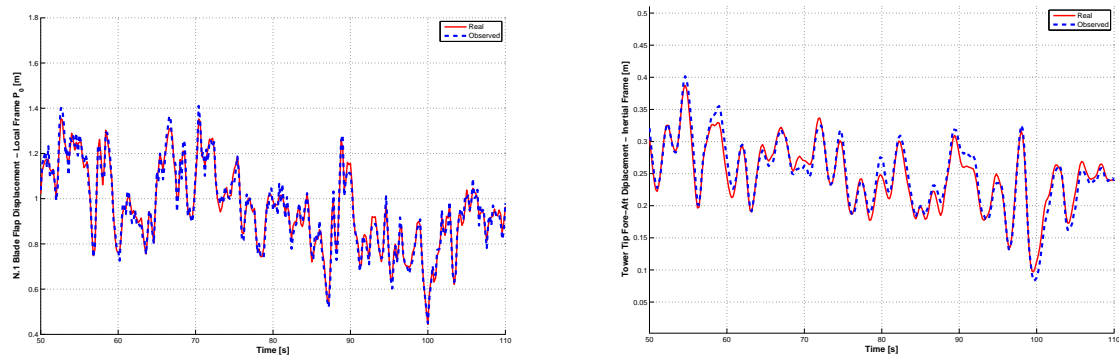


Fig. 7: Turbulent wind with 11 m/sec mean hub-height wind speed and Category A turbulence. Time history of blade (left) and tower (right) deflections. Real: solid line; observed: dashed line.

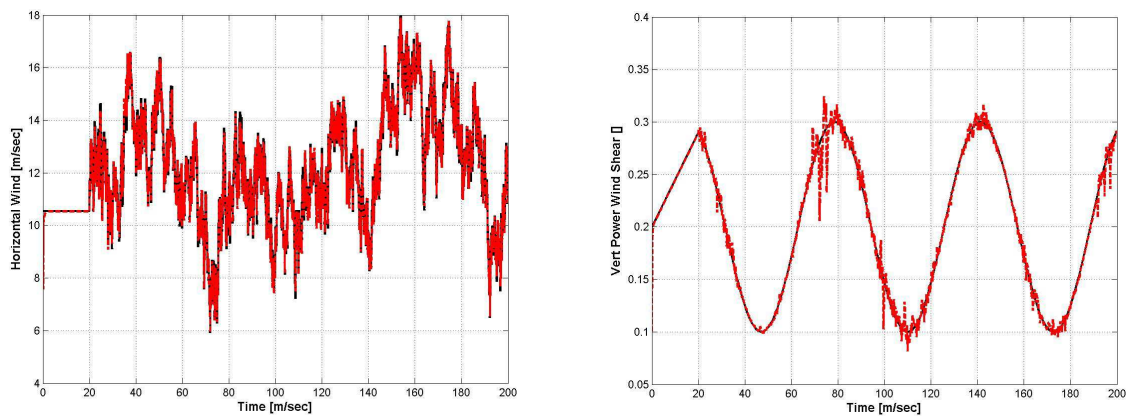


Fig. 8: Estimation of generalized wind states. Hub wind V_h (left) and power law exponent V_s (right). Real: solid line; observed: dashed line.

- [4] C.L. Bottasso, A. Croce, 'Advanced Control Laws for Variable-Speed Wind Turbines and Supporting Enabling Technologies', in preparation for submission, 2009.
- [5] X. Ma, *Adaptive Extremum Control and Wind Turbine Control*, Ph.D.thesis, Technical University of Denmark, 1997.
- [6] K.A. Myers, B.D. Tapley, 'Adaptive Sequential Estimation with Unknown Noise Statistics', *IEEE Transactions on Automatic Control*, **21**:520–523, 1976.
- [7] A.V. Oppenheim, R.W. Schaffer, *Discrete-Time Signal Processing*, Prentice-Hall, 1989, pp. 311-312.
- [8] K. Reif, R. Unbehauen, 'The Extended Kalman Filter as an Exponential Observer for Non-linear Systems', *IEEE Transactions on Signal Processing*, **47**:2324–2328, 1999.
- [9] K. Stol, G. Bir, NWTC Design Codes, <http://wind.nrel.gov/designcodes/simulators/symdyn/>, last modified May 26, 2005; accessed August 18, 2008.

-
- [10] D. Simon, *Optimal State Estimation: Kalman, H-infinity, and Nonlinear Approaches*, John Wiley & Sons, Inc., 2006.